Contribution from the Institut für Anorganische Chemie
and Laboratorium für Kristallographie, Universität Bern, CH-3000 Bern 9, Switzerland

# Mixed-Valence Ruthenium Dimers. Molecular and Electronic Structure of the *p*-Benzoquinone Diimine Bridged Ion $[(NH_3)_5Ru(bqd)Ru(NH_3)_5]^{5+}$ (bqd = *p*-Benzoquinone Diimine) and Its Relationship to the Creutz-Taube Ion

STEFAN JOSS,[1a] HANS BEAT BÜRGI,[1b] and ANDREAS LUDI*[1a]

*Received May 9, 1984*

Crystals of the mixed-valence ion $[(NH_3)_5Ru(bqd)Ru(NH_3)_5]^{5+}$ (bqd = *p*-benzoquinone diimine) were grown with *p*-benzenedisulfonate (salt I) and *m*-nitrobenzenesulfonate (salt II) as counterions. Crystal data for I: monoclinic, $P2_1/n$, 100 K, $a$ = 16.029 (4) Å, $b$ = 16.566 (5) Å, $c$ = 16.306 (7) Å, $\beta$ = 93.77 (3)°, $Z$ = 2. Crystal data for II: monoclinic, $P2_1/c$, $a$ = 8.402 (6) Å, $b$ = 25.535 (5) Å, $c$ = 28.918 (8) Å, $\beta$ = 91.92 (4)°, $Z$ = 4. The structure of I (100 K) was refined to $R$ = 3.3% for 6383 reflections with $F_o > 3\sigma(F_o)$, and the structure of II (295 K), to $R$ = 6.6% for 3792 reflections with $F_o > \sigma(F_o)$. Crystal I contains two crystallographically independent binuclear ions, both with symmetry $\bar{1}$; crystal II shows one $Ru^{II}Ru^{III}$ dimer of symmetry 1. The geometries of the independent dimers are the same within estimated standard deviations. Important distances are Ru—N(bridge) = 1.953 (2) Å, Ru—$NH_3$(trans) = 2.135 (2) Å, Ru—$NH_3$(cis) = 2.114 (1) Å, N=C = 1.341 (3) Å, C—C = 1.431 (2) Å, C=C = 1.356 (3) Å. The bridging ligand, which is planar to ±0.05 Å, bisects the *cis*-Ru-$NH_3$ bonds. The structural properties, the intense ($\epsilon$ = 108 000 $M^{-1}$ $cm^{-1}$) charge-transfer band, and the occurrence of three intervalence bands are compared to corresponding data for the Creutz-Taube ion and interpreted in terms of a symmetric ground state for both ions within the framework of a Hückel molecular orbital model.

## Introduction

Mixed-valence complexes continue to be a challenge for experimental as well as theoretical chemists.[2] The crucial issue of all of these investigations is the assessment of the degree of electronic coupling between the two ligand-bridged subunits. In terms of the popular Robin-Day classification[3] this issue is synonymous to the question whether a given mixed-valence compound can be characterized as "localized", class II, or "delocalized", class III. There is also the possibility that this classification is insufficient, in which case finer graduations might be necessary. The assignment will obviously be complicated by the time scale of the particular experimental technique used. Thus, the problem is best attacked by employing a variety of physical techniques and a critical synopsis of the various experimental results.

The prototype among binuclear mixed-valence complexes is undoubtedly the ($\mu$-pyrazine)decaammineruthenium(II,III) ion, the Creutz-Taube ion.[4] Considerable work has been devoted to the study of this ion, to its chemical and physical properties, and, in particular, to its intense and asymmetric near-infrared absorption band attributed to the intervalence electron transfer. In the course of our reinvestigation of the Creutz-Taube ion[5] we synthesized a mixed-valence dimer of two pentaammineruthenium moieties linked by *p*-benzoquinone diimine (bqd). As an uncomplexed species this diimine is easily hydrolyzed to the corresponding benzoquinone[6] whereas its ruthenium(II) complexes are stable, indicative of the prominent $\pi$-back-bonding capability of the Ru(II) $t_{2g}^6$ configuration.[7] A preliminary paper reported some spectroscopic properties of the novel ($\mu$-*p*-benzoquinone diimine)dekaammineruthenium(II,III) ion, $[(NH_3)_5Ru(bqd)Ru(NH_3)_5]^{5+}$.[8] The present paper describes its electronic absorption spectrum and molecular structure as determined by single-crystal X-ray diffraction and discusses their relationship to those of the Creutz-Taube ion.

Table I. Crystal Data for $[(NH_3)_5Ru(bqd)Ru(NH_3)_5]_2(C_6H_4S_2O_6)_5 \cdot 11H_2O$ (I) and $[(NH_3)_5Ru(bqd)Ru(NH_3)_5](C_6H_4(NO_2)SO_3)_5 \cdot 5H_2O$ (II)

| | I | | II |
|---|---|---|---|
| $T$, K | 100 | 295 | 295 |
| space group | $P2_1/n$ | | $P2_1/c$ |
| $a$, Å | 16.029 (4) | 16.044 (2) | 8.402 (6) |
| $b$, Å | 16.566 (5) | 17.126 (3) | 25.535 (5) |
| $c$, Å | 16.306 (7) | 16.399 (5) | 28.918 (8) |
| $\beta$, deg | 93.77 (3) | 93.93 (2) | 91.92 (4) |
| $V$, Å$^3$ | 4321 (4) | 4495 (3) | 6201 (7) |
| fw | 2336.4 | | 1579.5 |
| $Z$ | 2 | | 4 |
| $D_{measd}$ (flotation), g cm$^{-3}$ | | 1.73 (1) | 1.70 (1) |
| $D_{calcd}$, g cm$^{-3}$ | 1.796 | 1.726 | 1.692 |
| site sym of Ru dimer | $\bar{1}$ | | 1 |

## Experimental Section

**A. Preparation.** A slurry of 1.2 g (4.1 mmol) of $[Ru(NH_3)_5Cl]Cl_2$ in 45 mL of 0.1 mM HCl over 5 g of Zn amalgam produces a yellow solution of $Ru(NH_3)_5H_2O^{2+}$ (ca. 90 min). A 0.3-g (2 mmol) portion of *p*-phenylenediamine dihydrochloride is added, and the pH is adjusted to 7 with 2 M NaOH. After 30 min the greenish solution is filtered and oxidized at a constant potential of +50 mV vs. SSCE with Pt electrodes while the pH is kept at 7 ± 0.5 by addition of 0.5 M NaOH or 0.5 M HCl in small portions. The electrochemical oxidation lasts for approximately 2.5 h, consumes about 5.8 mF, and leads to an air-stable, very intensely blue solution of the mixed-valence ion:

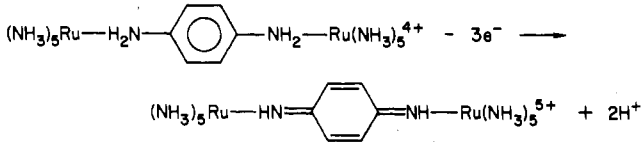


Argon is bubbled through the reaction solution during the entire preparation. A crude product (ca. 1 g) is precipitated by adding a saturated solution of 15 g of LiBr. Purification is achieved by chromatography: 6 L of an aqueous solution containing 1 g of crude product is pumped through a column of 25-mm diameter containing 30 g of Bio-Rex 70 in the protonated form (2 L h$^{-1}$, $P \approx 2$ bar). Violet mononuclear complexes are first eluted with 1 L of $H_2O$ and 1.5 L of 2 mM HCl, and the blue-green binuclear species, with ~2 L of 4 mM HCl. Freeze-drying of this solution yields about 560 mg of the chloride salt (0.85 mmol). From a stoichiometric mixture of aqueous solutions of this chloride salt and of $K_2C_6H_4S_2O_6$, potassium 1,4-benzenedisulfonate,[9] prismatic crystals are obtained by slow evaporation at 4 °C. Anal. Calcd for $[(NH_3)_5Ru(bqd)Ru(NH_3)_5]_2[C_6H_4O_6S_2]_5 \cdot 11H_2O$ (I): C, 21.59; H, 4.92; N, 14.39; S, 13.72. Found: C, 21.29; H, 5.17; N, 14.28; S, 14.05.

(1) (a) Institut für Anorganische Chemie. (b) Laboratorium für Kristallographie.
(2) Creutz, C. *Prog. Inorg. Chem.* **1983**, *30*, 1. Wong, K. Y.; Schatz, P. N. *Ibid.* **1981**, *28*, 370.
(3) Robin, M. B.; Day, P. *Adv. Inorg. Chem. Radiochem.* **1967**, *10*, 247.
(4) Creutz, C.; Taube, H. *J. Am. Chem. Soc.* **1969**, *91*, 3988; **1973**, *95*, 1086.
(5) (a) Fürholz, U.; Bürgi, H. B.; Wagner, F. E.; Stebler, A.; Ammeter, J. H.; Krausz, E.; Clark, R. J. H.; Stead, M. J.; Ludi, A. *J. Am. Chem. Soc.* **1984**, *106*, 121. (b) Fürholz, U.; Joss, S.; Bürgi, H. B.; Ludi, A., preceding paper in this issue.
(6) Corbett, J. F. *J. Chem. Soc. B* **1969**, 213. Nickel, U.; Kemnitz, K.; Jaenicke, W. *J. Chem. Soc., Perkin Trans 2* **1978**, 1188.
(7) Rieder, K.; Hauser, U.; Siegenthaler, H.; Schmidt, E.; Ludi, A. *Inorg. Chem.* **1975**, *14*, 1902.
(8) Joss, S.; Reust, H.; Ludi, A. *J. Am. Chem. Soc.* **1981**, *103*, 981.
(9) Fierz, H. E.; Stamm, G. *Helv. Chim. Acta* **1942**, *25*, 369.

0020-1669/85/1324-0949$01.50/0 

**Table II.** Intensity Collection and Refinement for I and II

| | I | II |
|---|---|---|
| cryst dimens, mm | 0.24 × 0.22 × 0.31 | 0.41 × 0.07 × 0.03 |
| $T$, K | 100 | 295 |
| lin abs coeff, $cm^{-1}$ | 10.0 | 7.4 |
| $2\theta$ limits, deg | 2-50 | 1-46 |
| scan width, deg | 1.3 + 0.35 tan $\theta$ | 1.1 + 0.35 tan $\theta$ |
| no. of unique reflcns measd | 7588 | 5555 |
| no. of unique reflcns | | |
| $F_o > 3\sigma(F_o)$ | 6383 | |
| $F_o > \sigma(F)$ | | 3792 |
| no. of parameters | 691 | 604 |
| $R$, % | 3.25 | 6.56 |
| $R_w$, % | 4.11 | 4.28 |

Needle-shaped crystals of the corresponding *m*-nitrobenzenesulfonate (Fluka) salt were obtained with an analogous preparative procedure. Anal. Calcd for $[(NH_3)_5Ru(bqd)Ru(NH_3)_5](C_6H_4NO_5S)_5 \cdot 5H_2O$ (II): C, 27.38; H, 4.21; N, 15.08; S, 10.15. Found: C, 27.34; H, 3.79; N, 14.98; S, 9.92.

Microanalyses were performed by CIBA Geigy, Basel. Spectra were measured on a Cary 17 DX.

**B. Collection and Reduction of Diffraction Data.** Lattice parameters for I (II) were determined by least-squares optimization of 22 (14) accurately centered reflections in the $\theta$ range between 13 and 18° (9.5 and 13°) with graphite-monochromatized Mo K$\alpha$ radiation ($\lambda$ = 0.71069 Å) and a CAD-4 diffractometer (Table I). Table II summarizes the conditions for data collection and details of refinement procedures. Three check reflections recorded every 180 min for both crystals did not show any systematic intensity fluctuations. Intensities were corrected for Lorentz-polarization effects but not for absorption. Neutral-atom scattering factors were employed including anomalous dispersion for all non-hydrogen atoms.[10] All calculations were performed on a IBM 3033 computer using the SHELX76 program system; ORTEP drawings were made with the XRAY76 system.

**C. Solution and Refinement of the Structures.** The structures of I and II were determined by Patterson and Fourier methods. For the study of I at 100 K hydrogen positions except those of the water molecules were obtained from difference Fourier maps and included in the final stage of the least-squares refinement with isotropic thermal parameters. A common isotropic temperature factor was assigned to all of the N-bonded hydrogens, another one to the carbon-bonded hydrogen atoms of the bridging ligand, and a third one to the hydrogens of the anion. Non-hydrogen atoms were refined anisotropically. For II, hydrogen positions, again without those of the water molecules, were included in the final cycles of the refinement. A fixed C–H and N–H distance of 0.89 Å was chosen. The ammonia molecules were allowed to adjust thier orientation around the Ru–N bonds with a fixed H–N–H angle of 109.5°. Anisotropic thermal motion was considered for Ru, the $SO_3^-$ and $NO_2$ groups, and the O atoms of the lattice water. Individual isotropic thermal parameters were assigned to the remaining non-hydrogen atoms, and a general isotropic temperature factor for the various groups of hydrogen atoms was refined as for I. The function $w(F_o - F_c)^2$ was minimized with $w = k/[(\sigma(I))^2 + 0.00003I^2]$ for I and $w = k/(\sigma(I))^2$ for II. Final $\Delta F$ maps showed residual electron density peaks smaller than 1.4 e/Å$^3$ in the neighborhood of S5 for I and 0.7 e/Å$^3$ around O95 for II. The final atomic coordinates are given in Tables III and IV. Listings of structure factors, thermal parameters, and hydrogen positions are available as supplementary material.

## General Description of the Structures

The 1,4-benzenedisulfonate salt of ($\mu$-*p*-benzoquinone diimine)dekaamminediruthenium(II,III) (I) shows two independent pairs of binuclear complex ions per unit cell, both with symmetry $\bar{1}$; i.e. the two ruthenium atoms in each dimer are equivalent by symmetry. The Ru–Ru axes of both dimers are approximately parallel to the 101 vector, but the orientations of their bridging ligand planes are different.

In the unit cell of the *m*-nitrobenzenesulfonate salt (II) the two ruthenium atoms of the four structurally equivalent dimers are not symmetry related, the site symmetry of the binuclear ion being only 1. The cations show different orientations and form sheets along the glide planes at $x$, $^1/_4$, $z$ and $x$, $^3/_4$, $z$. These sheets are separated by layers of the nitrobenzenesulfonate anions.

Both structures contain a highly complex network of hydrogen bonds involving the sulfonate groups, the coordinated ammonia, and the lattice water molecules. O–H–O and N–H–O distances range from 2.8 to 3.1 Å. The geometries of 1,4-benzenedisulfonate and *m*-nitrobenzenesulfonate do not show any unexpected features and do not require special comments. Their interatomic distances and angles are included in the supplementary material.

(10) "International Tables for X-ray Crystallography"; Kynoch Press: Birmingham, England, 1974.

**Table III.** Final Atomic Coordinates and $B_{eq}$ Values for I[a]

| atom | $x/a$ | $y/b$ | $z/c$ | $B_{eq}$ |
|---|---|---|---|---|
| Ru1 | 0.2943 (0) | 0.4287 (0) | 0.3216 (0) | 0.73 (1) |
| N11 | 0.3613 (2) | 0.4237 (2) | 0.4258 (2) | 1.00 (13) |
| N12 | 0.2189 (2) | 0.4236 (2) | 0.2083 (2) | 1.37 (16) |
| N13 | 0.4005 (2) | 0.4483 (2) | 0.2526 (2) | 1.24 (15) |
| N14 | 0.1856 (2) | 0.4064 (2) | 0.3840 (2) | 1.21 (14) |
| N15 | 0.3131 (2) | 0.3026 (2) | 0.3105 (2) | 1.23 (14) |
| N16 | 0.2668 (2) | 0.5530 (2) | 0.3286 (2) | 1.41 (16) |
| C11 | 0.4284 (2) | 0.4619 (2) | 0.4606 (2) | 1.15 (15) |
| C12 | 0.4622 (2) | 0.5334 (2) | 0.4271 (2) | 1.09 (15) |
| C13 | 0.5308 (2) | 0.5695 (2) | 0.4651 (2) | 1.10 (15) |
| Ru2 | 0.3044 (0) | 0.4140 (0) | 0.8184 (0) | 0.90 (1) |
| N21 | 0.4168 (2) | 0.4186 (2) | 0.8721 (2) | 1.29 (14) |
| N22 | 0.1862 (2) | 0.4086 (2) | 0.7520 (2) | 1.51 (16) |
| N23 | 0.2952 (3) | 0.5404 (2) | 0.8085 (2) | 1.63 (17) |
| N24 | 0.3062 (2) | 0.2862 (2) | 0.8215 (2) | 1.44 (16) |
| N25 | 0.3618 (2) | 0.4080 (2) | 0.7057 (2) | 1.23 (15) |
| N26 | 0.2402 (2) | 0.4135 (2) | 0.9277 (2) | 1.73 (16) |
| C21 | 0.4563 (2) | 0.4596 (2) | 0.9336 (2) | 1.08 (15) |
| C22 | 0.4142 (2) | 0.5143 (2) | 0.9846 (2) | 1.22 (15) |
| C23 | 0.4558 (2) | 0.5521 (2) | 1.0475 (2) | 1.64 (16) |
| S3 | 0.1880 (1) | 0.5180 (1) | 0.5678 (1) | 1.93 (4) |
| O31 | 0.2184 (2) | 0.4357 (2) | 0.5775 (2) | 2.27 (13) |
| O32 | 0.2316 (2) | 0.5646 (2) | 0.5088 (2) | 2.93 (15) |
| O33 | 0.1832 (2) | 0.5587 (2) | 0.6469 (2) | 2.42 (16) |
| C31 | 0.0826 (2) | 0.5077 (2) | 0.5290 (2) | 2.13 (17) |
| C32 | 0.0501 (3) | 0.5595 (2) | 0.4676 (2) | 2.39 (18) |
| C33 | −0.0331 (3) | 0.5516 (3) | 0.4397 (2) | 2.45 (18) |
| S4 | 0.0653 (1) | 0.2187 (1) | 0.2528 (1) | 0.98 (3) |
| O41 | 0.1351 (2) | 0.2635 (2) | 0.2889 (2) | 1.19 (13) |
| O42 | 0.0777 (2) | 0.1323 (2) | 0.2552 (2) | 3.47 (17) |
| O43 | −0.0134 (2) | 0.2397 (2) | 0.2856 (2) | 4.17 (16) |
| S5 | 0.0318 (1) | 0.2755 (1) | −0.1270 (1) | 2.07 (4) |
| O51 | 0.1156 (2) | 0.2868 (2) | −0.1541 (2) | 2.49 (16) |
| O52 | −0.0025 (2) | 0.1976 (2) | −0.1532 (2) | 1.64 (14) |
| O53 | −0.0265 (2) | 0.3410 (2) | −0.1475 (2) | 4.32 (17) |
| C41 | 0.0570 (2) | 0.2450 (2) | 0.1477 (2) | 1.06 (15) |
| C42 | 0.1267 (2) | 0.2317 (2) | 0.1022 (2) | 1.13 (16) |
| C43 | 0.1197 (2) | 0.2432 (2) | 0.0182 (2) | 1.43 (17) |
| C44 | 0.0439 (2) | 0.2700 (2) | −0.0188 (2) | 1.36 (17) |
| C45 | −0.0237 (2) | 0.2869 (3) | 0.0272 (3) | 2.06 (18) |
| C46 | −0.0168 (2) | 0.2733 (2) | 0.1114 (2) | 1.94 (18) |
| S6 | 0.3570 (1) | 0.2786 (1) | 0.0765 (1) | 1.19 (4) |
| O61 | 0.3349 (2) | 0.2271 (2) | 0.1439 (2) | 1.93 (12) |
| O62 | 0.3424 (2) | 0.3641 (2) | 0.0936 (2) | 1.68 (12) |
| O63 | 0.3203 (2) | 0.2546 (2) | −0.0031 (2) | 1.22 (11) |
| S7 | 0.7486 (1) | 0.2728 (1) | 0.0591 (1) | 1.21 (3) |
| O71 | 0.7705 (2) | 0.2253 (2) | −0.0114 (2) | 1.65 (11) |
| O72 | 0.7846 (1) | 0.2445 (2) | 0.1377 (2) | 1.74 (12) |
| O73 | 0.7645 (2) | 0.3592 (2) | 0.0465 (2) | 1.85 (12) |
| C61 | 0.4671 (2) | 0.2702 (2) | 0.0714 (2) | 1.47 (15) |
| C62 | 0.5182 (2) | 0.2776 (2) | 0.1429 (2) | 1.55 (16) |
| C63 | 0.6041 (2) | 0.2754 (2) | 0.1398 (2) | 1.07 (15) |
| C64 | 0.6386 (2) | 0.2659 (2) | 0.0647 (2) | 1.18 (15) |
| C65 | 0.5880 (2) | 0.2561 (2) | −0.0071 (2) | 1.37 (16) |
| C66 | 0.5013 (2) | 0.2577 (2) | −0.0039 (2) | 1.28 (15) |
| O91 | 0.3768 (2) | 0.5806 (2) | 0.6541 (3) | 7.01 (21) |
| O92 | −0.0833 (2) | 0.4624 (3) | 0.7344 (2) | 6.67 (20) |
| O93 | 0.0398 (3) | 0.5843 (3) | 0.7269 (3) | 5.71 (32) |
| O94 | 0.1977 (5) | 0.5880 (3) | 1.1193 (4) | 18.09 (44) |
| O95 | 0.1060 (3) | 0.5378 (3) | 0.8888 (4) | 11.14 (41) |
| O96 | −0.0420 (8) | 0.5022 (10) | 0.9685 (11) | 18.40 (132) |

[a] $B_{eq} = 8\pi^2/3\Sigma_i\Sigma_j U_{ij}$ where the general temperature factor expression is $\exp(-2\pi^2\{U_{11}h^2a^{*2} + U_{22}k^2b^{*2} + U_{33}l^2c^{*2} + 2U_{12}hka^*b^* + 2U_{13}hla^*c^* + 2U_{23}klb^*c^*\})$. Numbering scheme: cations, cf. Table V; anions, cf. supplementary material. Occupancy for O96, 0.5.

Table IV. Final Atomic Coordinates and $B_{eq}$ Values for II[a]

| atom | x/a | y/b | z/c | $B_{eq}$ | atom | x/a | y/b | z/c | $B_{eq}$ |
|---|---|---|---|---|---|---|---|---|---|
| Ru1 | 0.2921 (1) | 0.2854 (0) | 0.3242 (0) | 1.52 (5) | S5 | 0.9041 (4) | 0.2056 (1) | 0.2185 (1) | 2.08 (19) |
| N11 | 0.3542 (10) | 0.2544 (3) | 0.3838 (3) | 2.36 (20)* | O51 | 0.7845 (11) | 0.2242 (4) | 0.1855 (3) | 3.36 (54) |
| N12 | 0.2114 (11) | 0.3154 (3) | 0.2587 (3) | 2.65 (20)* | O52 | 1.0623 (10) | 0.2194 (4) | 0.2045 (3) | 3.39 (56) |
| N13 | 0.5272 (10) | 0.2844 (4) | 0.2992 (3) | 3.40 (22)* | O53 | 0.8758 (10) | 0.2200 (4) | 0.2657 (3) | 3.39 (58) |
| N14 | 0.0528 (10) | 0.2858 (4) | 0.3468 (3) | 3.07 (20)* | N5 | 0.6715 (15) | 0.0301 (5) | 0.1545 (4) | 2.60 (73) |
| N15 | 0.2617 (11) | 0.2087 (3) | 0.2983 (3) | 2.91 (21)* | O54 | 0.5932 (13) | 0.0554 (4) | 0.1265 (4) | 3.14 (68) |
| N16 | 0.3199 (11) | 0.3634 (3) | 0.3458 (3) | 3.06 (21)* | O55 | 0.6668 (15) | −0.0180 (4) | 0.1564 (4) | 3.86 (84) |
| Ru2 | 0.9388 (1) | 0.2214 (0) | 0.5633 (0) | 1.95 (5) | C51 | 0.8913 (15) | 0.1357 (5) | 0.2161 (4) | 2.82 (27)* |
| N21 | 0.8612 (10) | 0.2623 (3) | 0.5103 (3) | 1.93 (18)* | C52 | 0.7854 (15) | 0.1116 (5) | 0.1866 (4) | 2.75 (27)* |
| N22 | 1.0369 (12) | 0.1795 (4) | 0.6222 (3) | 3.46 (23)* | C53 | 0.7855 (16) | 0.0575 (5) | 0.1861 (5) | 2.89 (28)* |
| N23 | 0.7173 (10) | 0.2208 (4) | 0.5962 (3) | 2.83 (19)* | C54 | 0.8830 (15) | 0.0285 (5) | 0.2159 (4) | 2.87 (28)* |
| N24 | 1.1673 (10) | 0.2222 (4) | 0.5352 (3) | 2.96 (21)* | C55 | 0.9889 (18) | 0.0529 (5) | 0.2453 (5) | 3.69 (32)* |
| N25 | 1.0027 (10) | 0.2916 (3) | 0.5974 (3) | 2.70 (20)* | C56 | 0.9932 (17) | 0.1072 (5) | 0.2458 (5) | 3.63 (30)* |
| N26 | 0.8909 (11) | 0.1483 (3) | 0.5302 (3) | 3.03 (21)* | S6 | 1.0058 (5) | 0.1493 (1) | 0.4083 (1) | 3.26 (21) |
| C11 | 0.4747 (12) | 0.2587 (4) | 0.4151 (4) | 1.97 (22)* | O61 | 0.8484 (11) | 0.1584 (3) | 0.4245 (3) | 5.03 (58) |
| C12 | 0.5992 (12) | 0.2961 (4) | 0.4122 (3) | 2.23 (22)* | O62 | 1.0255 (13) | 0.1689 (4) | 0.3622 (4) | 7.77 (68) |
| C13 | 0.7233 (12) | 0.2966 (4) | 0.4434 (3) | 2.31 (23)* | O63 | 1.1286 (13) | 0.1654 (4) | 0.4405 (4) | 2.47 (72) |
| C21 | 0.7351 (12) | 0.2606 (4) | 0.4806 (4) | 1.79 (21)* | N6 | 0.8553 (20) | −0.0269 (6) | 0.3307 (5) | 4.75 (100) |
| C22 | 0.6090 (12) | 0.2237 (4) | 0.4843 (3) | 2.55 (22)* | O64 | 0.7559 (16) | −0.0039 (5) | 0.3089 (4) | 5.11 (83) |
| C23 | 0.4827 (12) | 0.2233 (4) | 0.4535 (3) | 2.27 (21)* | O65 | 0.8945 (18) | −0.0728 (5) | 0.3224 (4) | 5.26 (94) |
| S3 | 0.8161 (5) | 0.4108 (1) | 0.3047 (1) | 2.73 (21) | C61 | 1.0190 (17) | 0.0799 (6) | 0.4032 (5) | 3.54 (30)* |
| O31 | 0.9775 (12) | 0.3921 (4) | 0.3023 (3) | 4.58 (66) | C62 | 0.9345 (16) | 0.0550 (5) | 0.3692 (5) | 3.12 (28)* |
| O32 | 0.7156 (14) | 0.3757 (4) | 0.3274 (4) | 3.63 (74) | C63 | 0.9515 (17) | 0.0004 (5) | 0.3669 (5) | 3.34 (29)* |
| O33 | 0.7544 (12) | 0.4270 (4) | 0.2609 (3) | 4.76 (65) | C64 | 1.0442 (18) | −0.0276 (7) | 0.3962 (5) | 5.20 (38)* |
| N3 | 0.6932 (13) | 0.6056 (5) | 0.3396 (5) | 4.62 (74) | C65 | 1.1263 (21) | −0.0017 (7) | 0.4325 (6) | 6.04 (43)* |
| O34 | 0.6280 (13) | 0.6074 (4) | 0.3008 (4) | 6.50 (70) | C66 | 1.1123 (18) | 0.0533 (6) | 0.4357 (5) | 4.40 (36)* |
| O35 | 0.6970 (13) | 0.6428 (4) | 0.3666 (4) | 4.38 (67) | S7 | 0.4128 (6) | 0.1007 (2) | 0.5734 (2) | 5.21 (26) |
| C31 | 0.8253 (15) | 0.4670 (5) | 0.3407 (4) | 2.24 (26)* | O71 | 0.5523 (14) | 0.1173 (4) | 0.5510 (4) | 10.41 (84) |
| C32 | 0.7544 (14) | 0.5131 (5) | 0.3259 (4) | 2.35 (26)* | O72 | 0.2681 (14) | 0.1060 (5) | 0.5477 (6) | 9.50 (105) |
| C33 | 0.7649 (16) | 0.5561 (5) | 0.3543 (4) | 2.88 (28)* | O73 | 0.4061 (21) | 0.1249 (4) | 0.6182 (5) | 15.58 (113) |
| C34 | 0.8481 (16) | 0.5549 (5) | 0.3960 (5) | 3.38 (30)* | N7 | 0.6236 (23) | −0.0546 (7) | 0.6735 (6) | 7.86 (132) |
| C35 | 0.9196 (15) | 0.5092 (5) | 0.4107 (4) | 3.00 (28)* | O74 | 0.6657 (21) | −0.0975 (6) | 0.6757 (6) | 14.54 (131) |
| C36 | 0.9104 (16) | 0.4645 (5) | 0.3825 (4) | 3.36 (30)* | O75 | 0.6409 (26) | −0.0220 (7) | 0.7041 (6) | 8.31 (163) |
| S4 | 0.1441 (4) | 0.3768 (1) | 0.4762 (1) | 2.45 (18) | C71 | 0.4352 (16) | 0.0322 (5) | 0.5838 (5) | 3.35 (30)* |
| O41 | 0.0495 (10) | 0.4223 (4) | 0.4840 (3) | 4.67 (55) | C72 | 0.5153 (16) | 0.0166 (5) | 0.6238 (5) | 3.57 (31)* |
| O42 | 0.1255 (10) | 0.3364 (3) | 0.5104 (3) | 3.86 (51) | C73 | 0.5396 (18) | −0.0367 (6) | 0.6308 (5) | 4.18 (34)* |
| O43 | 0.1250 (12) | 0.3562 (4) | 0.4300 (3) | 2.65 (59) | C74 | 0.4883 (21) | −0.0730 (7) | 0.5991 (6) | 6.10 (43)* |
| N4 | 0.7012 (15) | 0.3747 (5) | 0.5585 (4) | 3.83 (74) | C75 | 0.4121 (19) | −0.0574 (6) | 0.5602 (6) | 5.32 (39)* |
| O44 | 0.6546 (12) | 0.3371 (4) | 0.5795 (3) | 4.35 (61) | C76 | 0.3849 (18) | −0.0036 (6) | 0.5509 (5) | 4.82 (37)* |
| O45 | 0.8295 (12) | 0.3955 (4) | 0.5663 (4) | 4.42 (69) | O91 | 0.4693 (12) | 0.2212 (5) | 0.2079 (3) | 5.23 (78) |
| C41 | 0.3436 (14) | 0.3978 (4) | 0.4817 (4) | 2.17 (24)* | O92 | 0.6592 (13) | 0.1815 (4) | 0.3346 (4) | 11.02 (76) |
| C42 | 0.4404 (14) | 0.3778 (5) | 0.5166 (4) | 2.49 (25)* | O93 | 0.7581 (16) | 0.3708 (5) | 0.1734 (4) | 6.70 (96) |
| C43 | 0.5940 (15) | 0.3958 (5) | 0.5204 (4) | 2.48 (24)* | O94 | 0.3536 (13) | 0.2334 (5) | 0.6274 (4) | 6.97 (92) |
| C44 | 0.6576 (17) | 0.4322 (5) | 0.4923 (4) | 3.57 (32)* | O95 | 0.4338 (14) | 0.4027 (6) | 0.2407 (5) | 14.44 (116) |
| C45 | 0.5570 (17) | 0.4524 (5) | 0.4571 (5) | 3.88 (33)* | | | | | |
| C46 | 0.4026 (15) | 0.4358 (5) | 0.4537 (4) | 2.76 (27)* | | | | | |

[a] See footnote of Table III. Starred values indicate those of atoms refined isotropically.

All three independent dimers show essentially the same general structure, which is illustrated by an ORTEP plot of ion 1 of crystal I (figure 1). The overall geometry of the complex ion is characterized by the trans arrangement of the two $Ru(NH_3)_5$ moieties about the bridging ligand. For all three dimers, the two $Ru(NH_3)_5$ subunits are eclipsed and the angle between the bridge plane and the *cis*-Ru–$NH_3$ bonds deviates less than 5° from 45°.

For the mononuclear precursor complex of Ru(II) the quinone form of the ligand has been inferred from spectroscopic and electrochemical studies.[7] Our crystal structure directly demonstrates that the bridging ligand is *p*-benzoquinone diimine. The six carbon atoms and the two nitrogens of the bridge form a planar molecule. The largest deviations from the least-squares plane are ±0.001 Å for the C13 atoms and ±0.015 Å for the C21 atoms (I) and 0.054 Å for N11 (II). The Ru atoms deviate between 0.05 and 0.27 Å, and the N atoms of the trans ammonia molecules, between 0.22 and 0.62 Å from this plane, corresponding to angles between the bridge plane and the N1–Ru–N2 line from 3.3 to 8.7°. The conformation of the bridging ligand can be described as "boat" for the noncentrosymmetric ion of II and as a symmetry-imposed "chair" for the two ions in I.

### Coordination Geometry and Bonding

Discussion of the coordination geometry in the mixed-valence dimer is based on data for three independent binuclear ions. Important interatomic distances, angles, and their mean values

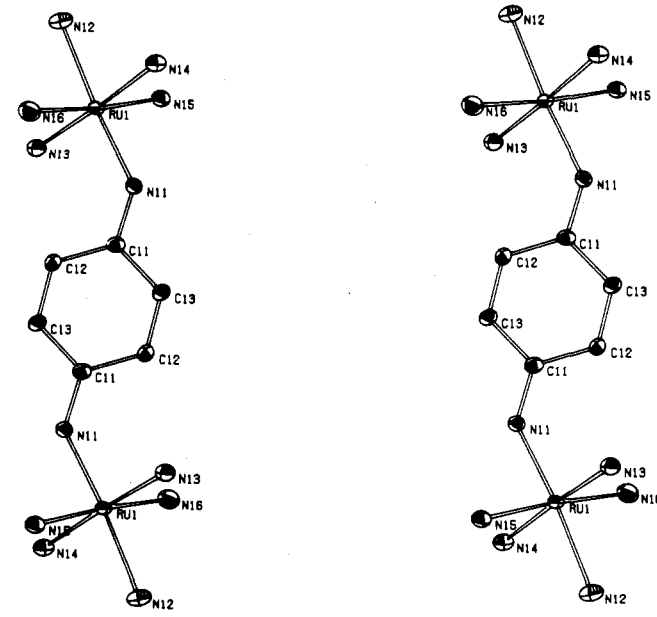


Figure 1. Stereoview of the $[(NH_3)_5Ru(bqd)Ru(NH_3)_5]^{5+}$ ion in the structure of I.

**Table V.** Selected Interatomic Distances (Å) and Angles (deg) for I and II

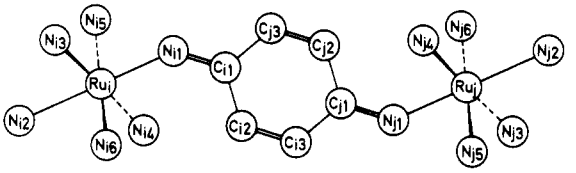


| | I | | II | | |
|---|---|---|---|---|---|
| | dimer 1 $i=j=1$ | dimer 2 $i=j=2$ | $i=1, j=2$ | $i=2, j=1$ | mean[a] |
| | | | Distances | | |
| Ru*i*–N*i*1 | 1.951 (3) | 1.952 (3) | 1.952 (9) | 1.949 (8) | 1.951 (2) |
| Ru*i*–N*i*2 | 2.142 (3) | 2.121 (3) | 2.133 (9) | 2.152 (9) | 2.133 (2) |
| Ru*i*–N*i*3 | 2.126 (3) | 2.105 (3) | 2.126 (9) | 2.118 (9) | 2.114 (1) |
| Ru*i*–N*i*4 | 2.107 (3) | 2.118 (3) | 2.135 (9) | 2.110 (9) | |
| Ru*i*–N*i*5 | 2.120 (3) | 2.111 (3) | 2.109 (8) | 2.107 (8) | |
| Ru*i*–N*i*6 | 2.111 (3) | 2.116 (3) | 2.098 (8) | 2.130 (8) | |
| N*i*1=C*i*1 | 1.341 (4) | 1.336 (5) | 1.340 (14) | 1.342 (14) | 1.339 (3) |
| C*i*1–C*i*2 | 1.426 (5) | 1.429 (5) | 1.421 (14) | 1.425 (14) | 1.431 (2) |
| C*i*1–C*j*3 | 1.436 (5) | 1.435 (5) | 1.432 (14) | 1.416 (14) | |
| C*i*2=C*i*3 | 1.364 (5) | 1.341 (5) | 1.356 (13) | 1.362 (13) | 1.353 (3) |
| | | | Angles | | |
| N*i*1–Ru*i*–N*i*2 | 175.2 (2) | 176.0 (4) | 176.1 (4) | 176.4 (4) | 175.6 (2) |
| N*i*1–Ru*i*–N*i*3 | 93.1 (1) | 93.1 (2) | 94.1 (3) | 94.7 (4) | 91.6 (1) |
| N*i*1–Ru*i*–N*i*4 | 89.8 (1) | 91.0 (1) | 87.6 (3) | 88.7 (4) | |
| N*i*1–Ru*i*–N*i*5 | 87.7 (1) | 87.1 (1) | 87.9 (3) | 89.2 (3) | |
| N*i*1–Ru*i*–N*i*6 | 95.7 (1) | 96.2 (1) | 95.6 (3) | 93.6 (3) | |
| N*i*3–Ru*i*–N*i*4 | 176.8 (3) | 175.7 (3) | 177.9 (5) | 176.0 (3) | 176.4 (2) |
| N*i*3–Ru*i*–N*i*5 | 89.0 (1) | 90.7 (1) | 88.3 (4) | 90.6 (3) | 91.2 (1) |
| N*i*3–Ru*i*–N*i*6 | 93.3 (1) | 91.9 (1) | 91.0 (4) | 92.3 (4) | |
| Ru*i*–N*i*1–C*i*1 | 136.8 (3) | 137.3 (3) | 137.5 (7) | 136.2 (7) | 137.0 (2) |
| N*i*1–C*i*1–C*i*2 | 123.0 (3) | 122.7 (3) | 123.8 (9) | 123.1 (9) | 122.9 (2) |
| N*i*1–C*i*1–C*j*3 | 119.6 (3) | 120.2 (3) | 119.1 (9) | 119.9 (9) | 119.9 (2) |
| C*i*2–C*i*1–C*j*3 | 117.4 (3) | 117.1 (3) | 117.0 (9) | 116.9 (9) | 117.2 (2) |
| C*i*1–C*i*2=C*i*3 | 120.3 (3) | 120.7 (3) | 121.2 (9) | 121.4 (9) | 120.6 (2) |
| C*j*1–C*i*3=C*i*2 | 122.2 (3) | 122.2 (3) | 122.2 (9) | 121.2 (9) | 122.2 (2) |

[a] Mean was calculated according to $\bar{x} = (1/\Sigma(\sigma x_i)^{-2})\Sigma x_i/(\sigma x_i)^2$, $\sigma\bar{x} = (\Sigma(\sigma x_i)^{-2})^{-1/2}$, $\sigma x_i$ representing the esd of an individual bond length.

**Table VI.** Comparison of Average Distances (Å) in Ruthenium Ammine Complexes with Pyrazine (pyz) and *p*-Benzoquinone Diimine (bqd)

| | Ru–N | Ru–$NH_3$ (trans) | Ru–$NH_3$ (cis) | ref |
|---|---|---|---|---|
| $Ru(NH_3)_6^{2+}$ | | 2.144 (4) | 2.144 (4) | *a* |
| $Ru(NH_3)_5pyz^{2+}$ | 2.006 (6) | 2.166 (7) | 2.153 (6) | *b* |
| $(NH_3)_5Ru(pyz)Ru(NH_3)_5^{4+}$ | 2.013 (3) | 2.149 (3) | 2.132 (5) | *c* |
| $(NH_3)_5Ru(pyz)Ru(NH_3)_5^{5+}$ | 1.991 (9) | 2.123 (7) | 2.112 (3) | *c* |
| $(NH_3)_5Ru(bqd)Ru(NH_3)_5^{5+}$ | 1.951 (2) | 2.133 (2) | 2.114 (1) | *d* |
| $(NH_3)_5Ru(pyz)Ru(NH_3)_5^{6+}$ | 2.115 (1) | 2.089 (1) | 2.101 (5) | *c* |
| $Ru(NH_3)_5pyz^{3+}$ | 2.076 (8) | 2.125 (8) | 2.106 (5) | *b* |
| $Ru(NH_3)_6^{3+}$ | | 2.104 (4) | 2.104 (4) | *a* |

[a] Stynes, H. C.; Ibers, J. A. *Inorg. Chem.* 1971, *10*, 2304. [b] Gress, M. W.; Creutz, C.; Quicksall, C. O. *Inorg. Chem.* **1981**, *20*, 1522. Refined without hydrogen atoms. [c] Reference 5b. [d] This work.

**Table VII.** Comparison of Interatomic Distances and HMO Bond Orders

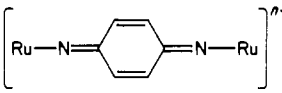


| | bond length, Å | | | bond order | | |
|---|---|---|---|---|---|---|
| | C=N | C–C | C=C | C=N | C–C | C=C |
| ligand[a] | 1.295 | 1.460 | 1.329 | 0.75 | 0.44 | 0.82 |
| $n=5$[b] | 1.341 (3) | 1.431 (2) | 1.356 (3) | 0.64 | 0.50 | 0.77 |

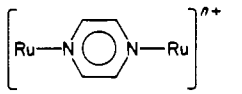


| | bond length, Å | | bond order | |
|---|---|---|---|---|
| | C–N | C–C | C–N | C–C |
| ligand[c] | 1.333 (1) | 1.388 (1) | 0.66 | 0.66 |
| $n=4$[d] | 1.353 (4) | 1.363 (5) | 0.64 | 0.67 |
| $n=5$[d] | 1.362 (4) | 1.361 (5) | 0.63 | 0.68 |

[a] Average from two determinations. Substituents on N: $SO_2CH_3$, $R = 5.3$ (Shvets, A. E.; Mishnev, A. F.; Bleidelis, Y. Y. *Zh. Strukt. Khim.* 1978, *19*, 544); β-naphthyl, $R = 3.6\%$ (Povet'eva, Z. P.; Chetkina, L. A.; Kopilov, V. V. *Zh. Strukt. Khim.* 1980, *21*, 118). [b] This work. [c] De With, G.; Harkema, S.; Feil, D. *Acta Crystallogr., Sect. B: Struct. Crystallogr. Cryst. Chem.* 1976, *B32*, 3178. Data: 184 K; $R = 7.1\%$. [d] Reference 5b.

are given in Table V; distances are virtually the same around all of the four distinguishable metal centers, namely dimers 1 and 2 in crystal I and the noncentrosymmetric dimer of crystal II. It is thus not possible to distinguish between Ru(II) and Ru(III); in other words the structural results imply equivalent metal centers in the mixed-valence dimer.

The molecular structure of the μ-*p*-benzoquinone diimine bridged diruthenium(II,III) dimer shows unmistakable signs of π-back-bonding from the $t_{2g}$(Ru) orbitals into a π* orbital of quinone diimine: The Ru–N(bridge) distance is shorter than in any comparable complex, and the difference between *cis*- and *trans*-Ru–$NH_3$ distances is largest (Table VI). The N=C, C=C, and C—C bonds of the bridge are lengthened and shortened, respectively, relative to those in simple organic derivatives of quinone diimine (Table VII). Analogous differences are observed between free pyrazine and the bridging ligand in the Creutz–Taube ion (Table VII).

All of these observations may be rationalized in terms of a simple Hückel molecular orbital model (HMO). HMO calcu-

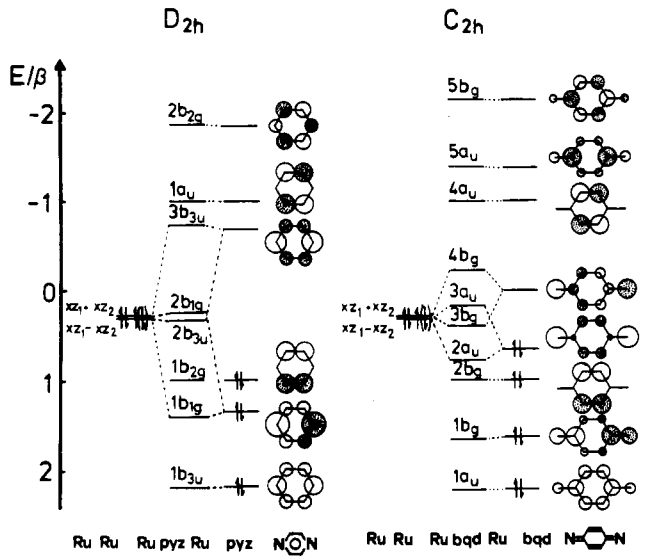


**Figure 2.** HMO diagram for $[(NH_3)_5Ru(L)Ru(NH_3)_5]^{4+/5+}$ (L = pyz, bqd): $z$ axis, Ru(bridge)Ru; $x$ axis, perpendicular to plane.

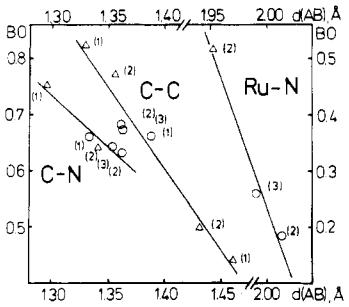


**Figure 3.** Correlation of the HMO bond orders to the experimental distances in $Ru(L)Ru^{n+}$: △, quinone diimine bridge; ○, pyrazine bridge. Key (cf. Table VII): (1) free ligand; (2) $n$ = 5; (3) $n$ = 4.

lations have been performed for symmetric dimers $(NH_3)_5Ru$-(bridge)$Ru(NH_3)_5$, assuming $\alpha(C) = 0$, $\beta(C-C) = \beta$, $\alpha(N) = 0.5\beta$, $\beta(C-N) = \beta$, $\alpha(Ru) = 0.3\beta$, and $\beta(Ru-N) = 0.3\beta$.[11] Corresponding MO schemes are shown in Figure 2: the HOMO and LUMO of uncomplexed quinone diimine are higher and lower, respectively, than those of uncomplexed pyrazine and therefore closer to the $d_{xz}$ orbital of Ru than in the Creutz–Taube complex. As a consequence, the mixing of ligand and metal $\pi$ orbitals is stronger and the calculated bond orders of Ru–N are higher for the quinone diimine [II,III] complex (0.54) than for the Creutz–Taube complex (0.28). Since the highest occupied MO of the dimer has a nodal plane between Ru and N, addition of an electron, producing the $Ru^{II}(L)Ru^{II}$ species, reduces the Ru–N bond order (0.37 for L = bqd, 0.20 for L = pyz). This agrees with the observed trend in bond lengths (Tables VI and VII).[12] Mixing of the LUMO of the bridge with $d_{xz}$ of Ru transfers electron density into the LUMO and changes the C–C and C–N bond orders in a way that is paralleled by experimental distances of the bridging ligands. The internal consistency of our calculations for two different complexes (Table VII) is illustrated by Figure 3, which correlates calculated bond orders with experimentally determined distances for symmetric Ru(bridge)Ru dimers.

We conclude that the structural data are satisfactorily accounted for by making the simplest possible assumption: The ground states for both pyrazine-bridged and quinone diimine bridged mixed-valence complex are symmetric (at least $\bar{1}$), owing to strong $t_{2g}$–$\pi^*$ back-bonding between Ru and the bridging molecule. Additional evidence to support this conclusion comes from the structure of II and of the tosylate salt of the Creutz–Taube ion.[5] In both compounds the two Ru centers of the dimer are not related by crystallographic symmetry; yet, the two Ru coordination geometries within a binuclear complex are closely similar to each other but distinctly different from those where genuine Ru(III) must be assumed (Table VI).

(11) $\beta$(Ru–N) was fixed at $0.3\beta$ according to the calculation of overlap integrals (cf. ref 13). The best consistency of the results for the different compounds was obtained for $\alpha(Ru) = 0.3\beta$.

(12) The bond orders calculated for the mononuclear $Ru(pyz)^{2+}$ (Ru–N = 0.22, C–N = 0.65, C–C = 0.68 Å) follow the same trend. Data for [III] and [III,III] are not included in our discussion because their electronic structure, i.e. the distribution of electrons in the d orbitals, is not known.

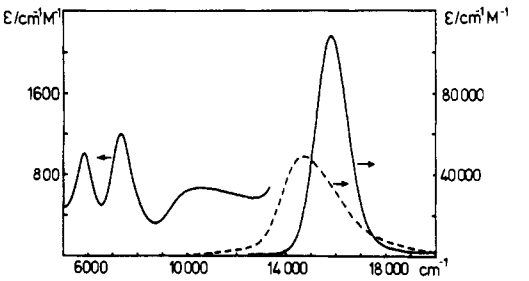


**Figure 4.** Absorption spectrum of the ion $[(NH_3)_5Ru(bqd)Ru(NH_3)_5]^{m+}$: solid line, $n$ = 5 (mixed-valence ion); broken line, $n$ = 4.

## Discussion of Electronic Properties

The most conspicuous feature in the optical spectrum of the quinone diimine bridged mixed-valence dimer is its very intense absorption band at 634 nm. To our knowledge, its extinction coefficient of 108 000 $M^{-1}$ $cm^{-1}$ is the highest reported so far for ruthenium complexes. The analogous band for the Creutz–Taube ion occurs at 565 nm with an intensity of 20 500 $M^{-1}$ $cm^{-1}$. In contrast to the behavior of other mixed-valence complexes of ruthenium the extinction coefficient of the band in the bqd-bridged complex decreases by a factor of about 2 upon reduction to the Ru(II)–Ru(II) dimer.[8] We assign this band to a metal-to-ligand charge-transfer transition, analogous to that in the Creutz–Taube ion. Our model predicts a relatively large difference in excitation energies between the two complexes, whereas the observed difference is rather small. The simple HMO approach, however, is based on $\pi$ orbitals only and on a very crude parameterization. It does not take into account electron–electron repulsion, configuration interaction, etc., all of which may influence the calculated excitation energies appreciably. It would thus seem satisfactory that the simple model reproduces the observed trend in excitation energies. The difference in intensity between the two mixed-valence complexes is in qualitative agreement with the different degrees of mixing between metal and bridge $\pi$ orbitals: high intensity for quinone diimine, i.e. a large degree of mixing of the orbitals involved, and vice versa for the Creutz–Taube complex.

A second unique property of the quinone diimine bridged species is the occurrence of three narrow and quite symmetric absorption bands at 950, 1360, and 1700 nm in the near-infrared region of the spectrum (Figure 4). These bands are an intrinsic property of the mixed-valence ion: They are of medium intensity, ($\epsilon \sim$ 1000 $M^{-1}$ $cm^{-1}$), their positions are independent of solvent, and they completely vanish upon reduction. For the Creutz–Taube complex, on the other hand, only one near-infrared band has been reported, peaking at 1570 nm.[4] Its asymmetric shape has been interpreted in terms of the vibronic coupling model[2b] assuming a noncentrosymmetric ground state with different Ru atoms albeit with only a small barrier for the degenerate rearrangement, i.e. for the exchange of the Ru atoms.

Recent spectroscopic work on single crystals presents evidence that the asymmetric near-infrared band of the Creutz–Taube ion contains two electronic transitions.[5] Work is in progress to verify (or disprove) a third weak infrared absorption ($\sim$5000 nm). The similar structural behavior of the quinone diimine bridged and the pyrazine-bridged diruthenium(II,III) dimer suggests a common interpretation of the near-infrared spectrum for both mixed-valence ions. The corresponding more detailed discussion of the available experimental evidence for the pyrazine-bridged and $p$-quinone diimine bridged mixed-valence species will be given in a forth-

coming paper.[13] It is based on a symmetric ion with two equivalent Ru centers and does include explicit consideration of the electronic structure of the bridge and of spin–orbit coupling. A straightforward interpretation of the near-infrared spectra containing more than one absorption band is not possible for the two ions within the framework of either the Hush model or the Hückel MO approach. Both descriptions allow for only one low-energy transition, the so-called "intervalence transition".

**Acknowledgment.** We thank Dr. H. Wagner, CIBA Geigy, Basel, for the elemental analyses. This work was supported by the Swiss National Science Foundation (Grant No. 2.209-0.81).

**Supplementary Material Available:** Listings of structure factors, thermal parameters, hydrogen positions, and bond lengths and angles for the anions of I and II and stereoviews of the unit cell of I and II (70 pages). Ordering information is given on any current masthead page.

(13) Joss, S.; Fürholz, U.; Hasselbach, K. M.; Bürgi, H. B.; Wordel, R.; Wagner, F. E.; Ludi, A., to be submitted for publication.

Contribution from the Department of Chemistry, University of California, Berkeley, California 94720

# Ferric Ion Sequestering Agents. 13. Synthesis, Structures, and Thermodynamics of Complexation of Cobalt(III) and Iron(III) Tris Complexes of Several Chelating Hydroxypyridinones[1]

ROBERT C. SCARROW, PAUL E. RILEY, KAMAL ABU-DARI, DAVID L. WHITE, and KENNETH N. RAYMOND*

*Received July 10, 1984*

Metal complexes of bidentate hydroxypyridinone ligands have been prepared and characterized. The pseudooctahedral Co(III) and Fe(III) tris complexes of 1-hydroxy-2(1*H*)-pyridinonate (1,2-opo) and the Fe(III) tris complex of 3-hydroxy-2(1*H*)-pyridinonate (3,2-opo) have been characterized by single-crystal X-ray diffraction. Variable-temperature NMR shows the cobalt complex is conformationally labile in $CDCl_3$. Determination of the formation constants of the Fe(III) complexes of several chelating hydroxypyridinone monoanions by spectrophotometric titration demonstrates that these ligands have chelation affinities for Fe(III) that are intermediate between those of monoanionic hydroxamate and dianionic catecholate species. The relatively strong acidities of the hydroxypyridinones ($pK_a$'s = 5–9) enable them to chelate ferric ion more effectively than catechol or hydroxamates in neutral or acidic solutions. The crystal structures of all the metal complexes are disordered with respect to the location of the nitrogen in the bidentate opo ligands. Two structurally similar forms of dark green Co(1,2-opo)$_3$ crystals were observed; one is $P2_1/n$ with $a$ = 9.702 (2) Å, $b$ = 9.516 (2) Å, $c$ = 17.146 (3) Å, $\beta$ = 103.41 (1)°, and $Z$ = 4, and the other is $C2/c$ with $a$ = 15.142 (2) Å, $b$ = 9.507 (1) Å, $c$ = 10.845 (1) Å, $\beta$ = 96.00 (1)°, and $Z$ = 4. Full-matrix least-squares refinement (on $|F|$) using 2589 and 882 reflections with $F_o^2 > 3\sigma(F_o^2)$ has converged with $R$ = 0.063 and 0.024 and $R_w$ = 0.071 and 0.031, respectively. Crystals of the tris complexes of Fe(III) with the 1,2-opo and 3,2-opo isomers form in space group $R\bar{3}c$. The Fe(1,2-opo)$_3$ complex crystallizes as yellow-orange parellelepipeds with $a = b$ = 9.634 (1) Å, $c$ = 31.290 (5) Å (hexagonal setting), and $Z$ = 6. Refinement using 556 reflections with $F_o^2 > 3\sigma(F_o^2)$ converged to $R$ = 0.021 and $R_w$ = 0.035. The Fe(3,2-opo)$_3$ complex forms as orange plates with $a = b$ = 9.782 (1) Å, $c$ = 29.615 (3) Å, and $Z$ = 6. Refinement using 629 observations with $F_o^2 > 3\sigma(F_o^2)$ converged to $R$ = 0.024 and $R_w$ = 0.035. Yellow-white needles of the uncomplexed molecule *N*,*N*-dimethyl-1-hydroxy-2-(1*H*)-pyridinone-6-carboxamide are of space group $P2_1/n$ with $a$ = 18.803 (2) Å, $b$ = 9.274 (1) Å, $c$ = 4.969 (1) Å, $\beta$ = 96.10 (1)°, and $Z$ = 4. Refinement using 1183 reflections with $F_o^2 > 3\sigma(F_o^2)$ converged to $R$ = 0.041 and $R_w$ = 0.061.

## Introduction

Siderophores are low-molecular weight compounds manufactured by microorganisms to facilitate the uptake of Fe(III), the concentration of which ($\sim 10^{-18}$ M) is severely limited by the extremely low solubility of ferric hydroxide ($K_{sp} \simeq 10^{-38}$) at physiological pH.[2] The most common functional groups of the siderophores are the hydroxamate (**1**) and catecholate (**2**) moieties,

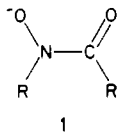


1

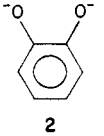


2

which act as strong bidentate chelating agents for Fe(III). In our efforts to design more effective sequestering agents for use in the treatment of human iron toxicity,[3] we and others have mimicked the efficient naturally occurring iron sequestering agents (such as enterobactin, the ferrichromes, and ferrioxamines) by incorporating catecholate and hydroxamate functionalities into synthetic macrochelating ligands.[4-6] These synthetic iron chelators have also proven useful in studies of the mechanisms of microbial iron uptake[7,8] and of iron removal from mammalian iron transport proteins.[4,9]

Recently we have begun investigation of other bidentate functional groups for possible use in siderophore-type complexing agents. This report describes the iron and cobalt complexes of several hydroxypyridinones ("Hopo's") in which the hydroxy group is ortho to the ketone functionality. The three unsubstituted chelating hydroxypyridinones and their abbreviations are shown in Figure 1. The deprotonated ligands will be abbreviated as "opo's": i.e., 1,2-opo$^-$, 3,2-opo$^-$, 3,4-opo$^-$.

(1) Previous paper in this series: Kappel, M. J.; Pecoraro, V. L.; Raymond, K. N. *Inorg. Chem.*, in press.
(2) Smith, R. M.; Martell, A. E. "Critical Stability Constants"; Plenum Press: New York, 1974–1977; Vol. 1–4.
(3) Martell, A. E., Anderson, W. F., Badman, D. G., Eds. "Development of Iron Chelators for Clinical Use"; Elsevier/North-Holland: 1981.
(4) Raymond, K. N.; Chung, T. D. Y.; Pecoraro, V. L.; Carrano, C. J. "The Biochemistry and Physiology of Iron"; Saltman, P., Hegenauer, J., Eds.; Elsevier Biomedical: New York, 1982; pp 649–662.
(5) Raymond, K. N.; Tufano, T. P. "The Biological Chemistry of Iron"; Dunford, H. B., Dolphin, D., Raymond, K. N., Seiker, L., Eds.; D. Reidel: Dordrecht, Holland, 1982; pp 85–105.
(6) Raymond, K. N.; Pecoraro, V. L.; Weitl, F. L. "Development of Iron Chelators for Clinical Use"; Martell, A. E., Anderson, W. F., Badman, D. G. , Eds.; Elsevier/North-Holland, 1981: pp 165–187.
(7) Heidinger, S.; Braun, V.; Pecoraro, V. L.; Raymond, K. N. *J. Bacteriol.* **1983**, *153*, 109–115.
(8) Raymond, K. N.; Müller, G.; Matzanke, B. F. *Top. Curr. Chem.* **1984**, *123*, 50–102.
(9) Rodgers, S. J.; Raymond, K. N. *J. Med. Chem.* **1983**, *26*, 439–442.

0020-1669/85/1324-0954$01.50/0 